34th Annual International Conference of the IEEE EMBS
San Diego, California USA, 28 August - 1 September, 2012

# Cell Tracking and Mitosis Detection using Splitting Flow Networks in Phase-Contrast Imaging

Amir Massoudi[1], Dimitri Semenovich[1] and Arcot Sowmya[1]

*Abstract*— **Cell tracking is a crucial component of many biomedical image analysis applications. Many available cell tracking systems assume high precision of the cell detection module. Therefore low performance in cell detection can heavily affect the tracking results. Unfortunately cell segmentation modules often have significant errors, especially in the case of phase-contrast imaging. In this paper we propose a tracking method that does not rely on perfect cell segmentation and can deal with uncertainties by exploiting temporal information and aggregating the results of many frames. Our tracking algorithm is fully automated and can handle common challenges of tracking such as cells entering/exiting the screen and mitosis events. To handle the latter, we modify the standard flow network and introduce the concept of a *splitting node* into it. Experiment results show that adding temporal information from the video microscopy improves the cell/mitosis detection and results in a better tracking system.**

## I. INTRODUCTION

Analysing cell movement and motility is an important part of many biological studies including cancer research and drug discovery [1], [2]. This is because most active cellular behaviours and functions involve movement. Manual analysis and observation of cellular images is an error prone task and requires long periods of tedious effort, as each image often contains hundreds of cells. A reliable automated tracking system can reduce human errors and speed up the image analysis. Design of an automated tracking system is an ongoing interest in computer vision [1], [2], [3], [4], [5], [6], [7], [8], [9].

A successful tracking system should address the common challenges of cell tracking, including cells entering/exiting the screen and mitosis events. Although numerous techniques have been proposed for cell tracking, tracking algorithms maybe classified into two main groups: tracking by model evolution and tracking by data association [1].

In tracking by model evolution, cell trajectories are computed by fitting a model around cells. This is achieved by minimizing an energy function, and the solution is then propagated to the next frame as an initial point of the optimization [1], [3], [4], [5], [6]. Active contours and level sets are the two main algorithms successfully used in this group. Active contours require special treatment for handling mitosis events due to their limitations in dealing with topological changes [4]. On the other hand, level sets are far more adaptable to topological changes and have been used extensively. However both algorithms suffer from the local optima problem and are not able to incorporate temporal information to improve tracking results. Moreover the system needs to evolve the cell models on each frame, which makes them computationally expensive.

In tracking by data association, cells are first detected in each frame and then individual cells are associated with each other. Association is performed based on features such as intensity or their relative spatial location [2], [7], [8]. When addressing the general data association problem, there are two main approaches. The first is to detect objects in individual frames and then connect the most likely objects to each other [10]. The drawback of this method is that it makes a strong assumption on the correct outcome of object detection and cannot deal with uncertainties. The second approach is to discretise the tracking area. Each discretised location will represent the probability of the object being in that location. This framework enables the tracking algorithm to deal with detection noises [10], [11].

Padfield et al.[2], introduce the coupling minimum-cost flow tracking algorithm that associates detected cells in two frames in fluorescent microscopy. The authors suggest modelling the tracking problem as a graph matching problem. Unfortunately this method requires a very good detection algorithm to detect cells in almost all frames, which is difficult to achieve in phase-contrast microscopy because of their poor image quality. Moreover it solves the problem using two frames at a time and does not incorporate the temporal information available in video microscopy to improve the results. Thus any error of the cell detector will compromise the tracking result.

In this paper we propose a tracking algorithm that does not require a perfect detection module. In fact it does not even require the detection module to return individual cells, and only needs probabilities or potentials that represent cell positions. Unlike other tracking algorithms that require user interaction or the number of cells a priori [4], [6], the proposed method is fully automatic and the number of cells can be inferred from the tracking results. The algorithm exploits temporal information to improve the tracking outcome and incorporates that information to detect mitosis events. It addresses the problem of cells entering/exiting the screen with a simple formulation, based on concepts defined by Berclaz et al. for multiple object tracking [11].

[1]School of Computer Science and Engineering, University of New South Wales, Sydney, New South Wales 2052, Australia. amirm,dimitris,sowmya at cse.unsw.edu.au

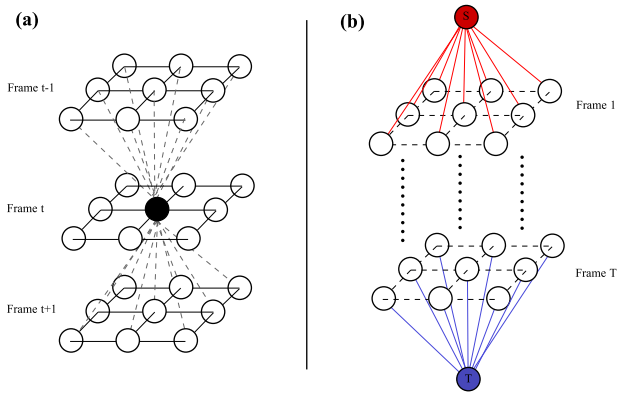


Fig. 1: (a) Shows three frames stacked together, the black filled node shows $x_i^t$ and the edges from and to this node are the reachable locations (b) shows the source $\mathcal{S}$ and sink $\mathcal{T}$ nodes, all the nodes of the first frame are connected to the source node and all the nodes of the last frame are connected to the sink node.

The main contributions of this paper are: extending the network flow tracking algorithm for cell analysis that also handles cells entering/exiting the screen, adding *splitting node* to the standard network flow formulation to handle cell division, and computing cell potentials along with cell mitosis potentials for setting edge weights of the network flow.

In what follows, a brief description of tracking with flow network is given in section II-A. We then introduce the concept of a splitting node in section II-C. Cell and mitosis detection modules are described in II-D, II-E respectively. Finally the result of the algorithm is shown in section III.

## II. APPROACH AND METHODS

For a tracking algorithm that deals with the uncertainties, noise and errors from cell segmentation, we develop a model following Berclaz et al. who introduced a multi-target tracking algorithm for pedestrian tracking [11]. Tracking is modelled as a network flow problem and is formulated as simple linear programming. We describe the tracking framework in II-A. In II-D we show how to set the edge weights of the flow network for microscopic images. Finally in II-B and II-C, the original tracking framework is extended to handle cells entering/exiting the screen and mitosis events respectively.

### A. Tracking with Network Flow

At first the tracked region in each frame is sampled into $K$ spatial locations on a regular grid. The grid cell size is set to the diameter of the average cell nucleus. To model object occupancy over $T$ frames, the frames are stacked together and a graph with $T \times K$ nodes is created (see Fig. 1). Each node $x_i^t$ of this graph denotes the probability or the potential of a cell being at position $i$ at time (frame) $t$. Accordingly an edge $f_{i,j}^t$ between two nodes $x_i^t$ and $x_j^{t+1}$ can be interpreted as a cell moving from location $i$ at time $t$ to a reachable location $j$ at time $t+1$. A set of reachable locations for an object at location $k$ is defined in a neighbourhood $\mathcal{N}(k) \subset \{1,\ldots,K\}$. In other words $\mathcal{N}(k)$ is the set of locations that the object can reach in the next time frame from location $k$.

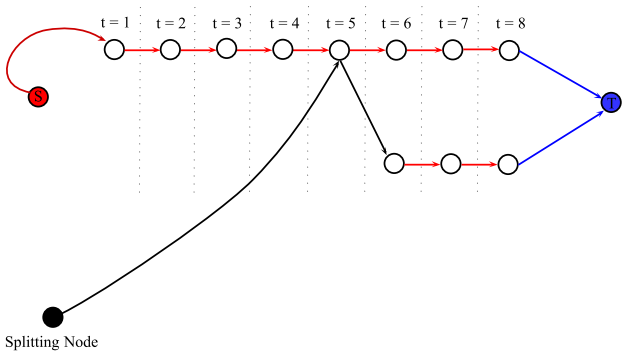


Fig. 2: The tracking output of the Fig.3. The splitting node injects the flow at time $t = 5$.

As shown in Fig. 1 (b), two special nodes ($\mathcal{S}$,$\mathcal{T}$) are added to the flow network. *Source node* $\mathcal{S}$ is connected to all the nodes of the first frame and can initiate a track by emitting flows. Each flow is then passed on to any of the neighbouring nodes of the next frame, and this continues until the flow reaches the last frame and gets injected to the *sink node* $\mathcal{T}$. Thus the sink node terminates the tracks. This flow can be modelled by the following linear programming equations [11]:

$$\underset{f}{\text{maximize}} \quad \sum_{i,t,j\in\mathcal{N}(i)} C_{i,j}^t . f_{i,j}^t \tag{1}$$

$$\text{subject to} \quad \forall\, i,j,t, \quad f_{i,j}^t \geq 0 \tag{2}$$

$$\forall\, t,i, \quad \sum_{j\in\mathcal{N}(i)} f_{i,j}^t \leq 1 \tag{3}$$

$$\forall\, t,j, \quad \sum_{i:j\in\mathcal{N}(i)} f_{i,j}^{t-1} = \sum_{k\in\mathcal{N}(j)} f_{j,k}^t \; . \tag{4}$$

In the objective function (1), $C_{i,j}^t$ is the cell occupancy potential that is assigned to each edge and indicates how likely it is to be part of a cell track. We describe how to compute this value later in section II-D. Constraints (2) and (3) make sure that no more than one object occupies the same location at the same time. Equation (4) imposes the flow conservation and continuity constraint and ensures that the total sums of the input and output flows are equal at all nodes.

The solution of the optimization problem is often integer, with $f_{i,j}^t \in \{0,1\}$ [12], [11]. Active flows running through the nodes indicate the possible location of each cell and the number of cells can be computed by counting the number of tracks resulting from the flow network. As an example, the resulting flow network of Fig. 3 is shown in Fig. 2.

The benefit of using this model is that it aggregates the results of all frames and makes a global decision rather than propagating the result of each frame to the next. This makes the algorithm less vulnerable to the errors of the cell detection module.

### B. Cells Entering/Exiting the Screen

The network flow formulation can successfully track those cells that are visible in the first frame and continue to persist

in the tracking region until the last frame. This is because the source and sink nodes are connected to the nodes of the first and the last frames respectively. However, if a cell enters the screen after the first frame, the optimization process might ignore the new cell completely or select an incorrect location in the previous frames to maximize the objective function. This is also the case when a cell exits the tracking region before the last frame.

To address this problem, we add two extra edges ($f_{S,i}$ , $f_{i,\mathcal{T}}$) to the neighbourhood of all nodes located on the image boundaries. $f_{S,i}$ makes it possible for the algorithm to start a new track at location $i$ to handle cells entering the screen. Edges $f_{i,\mathcal{T}}$ can terminate a track when a cells leaves the screen.

### C. Splitting Node Extension

One of the main challenges of a cell tracking system is to handle mitosis events, in which a parent cell divides into two daughter cells. Before splitting, a parent cell becomes rounder and brighter compared to its normal state, which is shown in Fig 3.

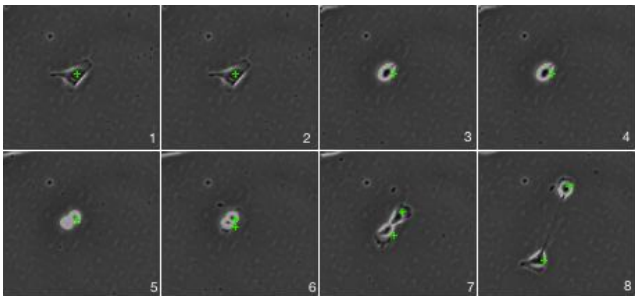


Fig. 3: Cell mitosis cycle along with tracking result, shown as a green plus. The algorithm detects the cell division in frame 6 and adds a second cross.

The flow conservation constraint in (4) does not allow outgoing flows to exceed the incoming flows and therefore does not allow a track to split and follow the two daughter cells after mitosis. To address this issue, we add a special node to the flow network called *Splitting Node*. A splitting node works exactly like a secondary source node, and can emit flows and is connected by the edge ($f_{\text{splitting},i}$) to any node $i$ that does not belong to the first and the last frames. Any emission from the splitting node will force the network to initiate another path according to constraint (4). To suppress unwanted emissions from a splitting node, each edge $f_{\text{splitting},i}$ is weighted with a value $M_i^t$, that is mitosis occurrence potential. We describe how to compute this value in section II-E. To model the splitting node, we reformulate the standard network flow linear programming problem as follows :

$$\underset{f}{\text{maximize}} \quad \sum_{i,t,j\in\mathcal{N}(i)} C_{i,j}^t . f_{i,j}^t + M_i^t . f_{\text{splitting},i}^t \qquad (5)$$

$$\text{subject to} \quad \forall\, i,j,t, \quad f_{i,j}^t \geq 0 \qquad (6)$$

$$\forall\, t,i, \quad \sum_{j\in\mathcal{N}(i)} f_{i,j}^t - f_{\text{splitting},i}^t \leq 1 \qquad (7)$$

$$\forall\, t,j, \quad \sum_{i:j\in\mathcal{N}(i)} f_{i,j}^{t-1} = \sum_{k\in\mathcal{N}(j)} f_{j,k}^t \ . \qquad (8)$$

The main difference of this formulation compared to that described in section II-A is in the objective function (5) and the new constraint (7). Flows originating from the splitting node are introduced while keeping the occlusion assumption.

The advantage of this method for detecting mitosis events is that the algorithm makes a decision by optimizing globally across all frames. Therefore if the mitosis detector produces a false positive result, the algorithm will often suppress the decision if it is not consistent with other evidence. Also if the detector does not detect the mitosis, the network will force the splitting node to create a new path if the new path can increase the objective function value.

### D. Cell Occupancy Potentials

To determine the likelihood that a node in the network might contain a cell, we measure the cell occupancy potential $C_{i,j}^t$, used in (1) . In order to compute it, first cell regions are distinguished from background regions using the method previously proposed [9]. Then distance transform is computed on the resulting mask and the outcome is stored in $D^t$ ($t$ indexes the frame number). As the nucleus of a cell is often located at its centre, $D^t$ has high values for the nucleus, smaller values for its cytoplasm and zero values for the background. $D^t$ is normalized adaptively by the maximum depth of each connected component individually and any value less than $d_t$ is suppressed (we set $d_t = 0.7$ empirically). Finally the value of the cell occupancy potential $C_{i,j}^t$ is calculated as follows:

$$\psi(i,j,t) = \max_{(m,n)\in Z(i)} (D_{(m,n)}^t) + \max_{(m,n)\in Z(j)} (D_{(m,n)}^{t+1}) \ , \qquad (9)$$

$$C_{i,j}^t = \log\left(\frac{\psi(i,j,t)}{1-\psi(i,j,t)}\right) . \qquad (10)$$

In (9), $Z(i)$ is a set of original image pixels mapped to spatial location $i$. Heuristically, $C_{i,j}^t$ will have negative values when the probability of a cell being at location $(i,j)$ is low.

### E. Mitosis Occurrence Potentials

To approximate the mitosis occurrence potentials $M_i^t$ used in (5), we train a logistic regression classifier on the histogram of gradients (HOG) of cells in their normal state and their mitosis state, on a window of size $S_m$ ($S_m$ is the average size of cells in mitosis state). For computing $M_i^t$, a window of the same size is centred at location $i$ of the original image and the corresponding sub-image is passed on to the logistic regression classifier. Because of the probabilistic nature of logistic regression, we can use the same formula that was mentioned in section II-D to set the weight of the splitting edges.

## III. RESULTS

We tested the splitting flow network tracking algorithm on a video with 122 frames (frame size $650 \times 515$) with 42 mitosis events. Our experiments showed that incorporating temporal information improves the cell detection, tracking and mitosis detection significantly. To quantitatively evaluate the mitosis detection, we compare the number of detected

mitosis events using logistic regression classifier with no temporal information, and the number of detected mitosis events using the splitting flow network. To accomplish this, mitosis classifier results are computed on a window of size $S_m$ centred around each cell pixel as described in II-E.
Let $I_c^t$ be the result of the mitosis classifier on all cell pixels in frame $t$. A mitosis mask $I_m^t$ is created by thresholding the resulting classifier image ($I_m^t = I_c^t \geq \lambda$, where $\lambda$ is the threshold). The noise in the resulting mask is removed by suppressing all connected components that are smaller than $\frac{S_m}{2}$. The outcome is then compared to a ground truth image labelled by an expert. Mitosis events are labelled in the ground truth images only once and exactly before the cells split. If the logistic regression classifier returns a positive response in any of $\{I_m^{t-2}, I_m^{t-1}, I_m^t\}$ frames and there is a labelled mitosis event in frame $t$, then the classifier output is considered to be true positive.

To compare the results, the receiver operating characteristic (ROC) curve of the logistic regression with different values of $\lambda$ is drawn. The fraction of true and false positives of mitosis detection using splitting flow network outcome is also computed. As shown in Fig. 4, mitosis detection using the splitting flow network outperforms the logistic regression classifier (for 24 true positives, logistic regression mitosis classifier produces 287 false positives while mitosis detection using network flow produces 20, which is 14 times fewer than the logistic regression classifier). The number of mitosis events detected by the splitting flow network is a function of the parameters $C_{i,j}^t$ and $M_{i,j}^t$ and the result shown in Fig. 4 corresponds to the specific values of these variables chosen. In principle different methods of calculating these parameters may generate different points.

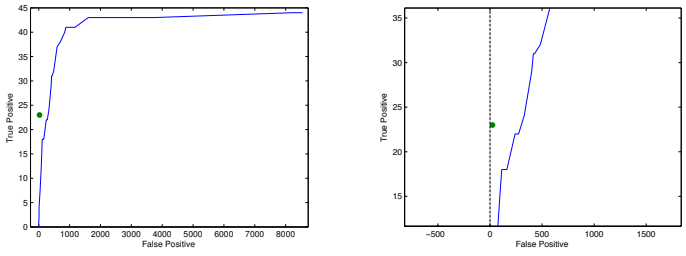


(I) ROC Curve (II) ROC Curve Zoomed In

Fig. 4: ROC curve for different values of $\lambda$. The filled green dot shows the result of mitosis detection using temporal information.

## IV. CONCLUSIONS

In this paper we have proposed an automatic cell segmentation algorithm that does not rely on a perfect segmentation module. The algorithm can track cells that enter or exit the screen and can also handle cell division, using splitting nodes added to the network flow graph. The tracking framework is not dependent on a particular cell detection technique and can use any cell detection algorithm that computes the required cell potentials. The algorithm still cannot handle cell occlusion. Occlusion happens when the flows merge together at a node in the graph. The algorithm cannot distinguish between selected occluded cells. Future work includes an automatic post processing step that traverses the resulting tracking network and prunes the occluded edges.

## V. ACKNOWLEDGMENT

We thank Dr William E. Hughes and Dr Katarina Mele of Garvan Institute of Medical Research[1] for providing the required data and for discussions on the subject.

## REFERENCES

[1] K. Li, E. D. Miller, M. Chen, T. Kanade, L. E. Weiss, and P. G. Campbell, "Cell population tracking and lineage construction with spatiotemporal context," *Medical Image Analysis*, vol. 12, no. 5, pp. 546–566, Oct. 2008. [Online]. Available: http://www.sciencedirect.com/science/article/B6W6Y-4SSNDBD-3/2/afdb1783e056f56d8d0a52faa7e39ab2

[2] D. Padfield, J. Rittscher, and B. Roysam, "Coupled minimum-cost flow cell tracking for high-throughput quantitative analysis," *Medical Image Analysis*, vol. 15, no. 4, pp. 650–668, Aug. 2011. [Online]. Available: http://www.sciencedirect.com/science/article/pii/S1361841510000988

[3] M. Tscherepanow, F. Z\llner, M. Hillebrand, and F. Kummert, "Automatic segmentation of unstained living cells in bright-field microscope images," *Advances in Mass Data Analysis of Images and Signals in Medicine, Biotechnology, Chemistry and Food Industry*, p. 158172, 2008.

[4] C. Zimmer, E. Labruyere, V. Meas-Yedid, N. Guillen, and J. Olivo-Marin, "Segmentation and tracking of migrating cells in videomicroscopy with parametric active contours: a tool for cell-based drug testing," *Medical Imaging, IEEE Transactions on*, vol. 21, no. 10, pp. 1212–1221, 2002.

[5] F. Yang, M. A. Mackey, F. Ianzini, G. Gallardo, and M. Sonka, "Cell segmentation, tracking, and mitosis detection using temporal context," in *Medical Image Computing and Computer-Assisted Intervention MICCAI 2005*, J. S. Duncan and G. Gerig, Eds. Berlin, Heidelberg: Springer Berlin Heidelberg, 2005, vol. 3749, pp. 302–309. [Online]. Available: http://www.springerlink.com/content/edtqflefe04xna8h/

[6] O. Debeir, P. Van Ham, R. Kiss, and C. Decaestecker, "Tracking of migrating cells under phase-contrast video microscopy with combined mean-shift processes," *Medical Imaging, IEEE Transactions on*, vol. 24, no. 6, pp. 697–711, 2005.

[7] Y. Chen, E. Ladi, P. Herzmark, E. Robey, and B. Roysam, "Automated 5-D analysis of cell migration and interaction in the thymic cortex from time-lapse sequences of 3-D multi-channel multi-photon images," *Journal of Immunological Methods*, vol. 340, no. 1, pp. 65–80, Jan. 2009. [Online]. Available: http://www.sciencedirect.com/science/article/pii/S0022175908003086

[8] S. Hadjidemetriou, B. Gabrielli, K. Mele, and P. Vallotton, "Detection and tracking of cell divisions in phase contrast video microscopy," *Proc. of the Third MICCAI Worshop on Microscopic Image Analysis with Applications in Biology*, 2008.

[9] A. Massoudi, A. Sowmya, K. Mele, and D. Semenovich, "Employing temporal information for cell segmentation using max-flow/min-cut in phase-contrast video microscopy," in *2011 Annual International Conference of the IEEE Engineering in Medicine and Biology Society,EMBC*. IEEE, Sep. 2011, pp. 5985–5988.

[10] A. Andriyenko and K. Schindler, "Multi-target tracking by continuous energy minimization," in *2011 IEEE Conference on Computer Vision and Pattern Recognition (CVPR)*. IEEE, Jun. 2011, pp. 1265–1272.

[11] J. Berclaz, F. Fleuret, and P. Fua, "Multiple object tracking using flow linear programming," in *Performance Evaluation of Tracking and Surveillance (PETS-Winter), 2009 Twelfth IEEE International Workshop on*, 2009, pp. 1–8.

[12] A. Andriyenko and K. Schindler, "Globally optimal multi-target tracking on a hexagonal lattice," in *Computer Vision ECCV 2010*, K. Daniilidis, P. Maragos, and N. Paragios, Eds. Berlin, Heidelberg: Springer Berlin Heidelberg, 2010, vol. 6311, pp. 466–479. [Online]. Available: http://www.springerlink.com/content/bwx8w5l052h77633/

[1]Garvan Institute of Medical Research, 384 Victoria Street, Sydney, New South Wales 2010, Australia.